

Probing magnetic structure with 3D sensitivity using polarized SANS

**Kathryn Krycka, Julie Borchers, Wangchun Chen, Shannon Watson,
Mark Laver, Thomas Gentile (NIST Center for Neutron Research)**

Ryan Booth, Charles Hogg, Sara Majetich (Carnegie Mellon University)

Yumi Ijiri, Sydney Harris, Liv Dedon (Oberlin College)

Jim Rhyne (LANSCCE, Los Alamos National Laboratory)

NCNR Summer School May 13, 2010

- **Motivation for studying 9 nm Fe_3O_4 nanoparticles**
- **Benefits of polarization-analyzed SANS**
- **Data and modeling at high field → canted magnetic shell**

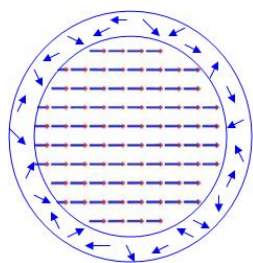
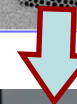
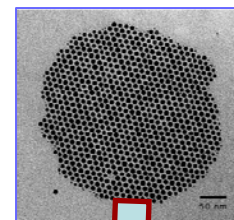
- **Altering magnetic shell thickness by:**
 - Varying temperature at high field**
 - Varying field at very low temperature**
 - Removing field and interparticle correlations**

- **Summary of results**

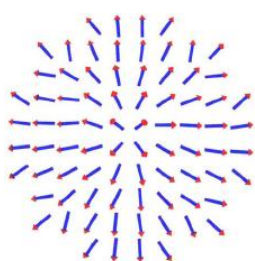
➤ Magnetic particles are promising for data storage and biomedical applications. However, precise determination of internal spin structure and interparticle coupling is elusive.

➤ Monodisperse, 9 nm, ferrimagnetic magnetite (Fe_3O_4) particles¹ crystallize into a face-centered cubic crystallites $\approx \mu\text{m}$. These crystallites are randomly oriented and form a powder. Magnetite in particular is biocompatible, stable, and has a moment comparable to Ni.

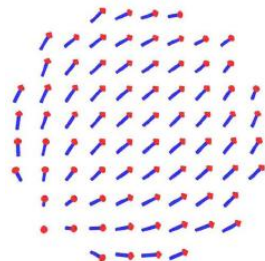
➤ Theoretical models suggest surface disorder² produces a magnetically dead (spin-glass) layer. Inclusion of surface anisotropy³ has led to differing predictions of hedgehog, artichoke, or throttled configurations. Either approach could account for the reduced moment experimentally observed with bulk probes.



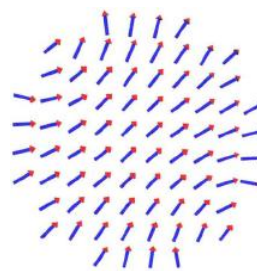
Disordered



Hedgehog



Artichoke

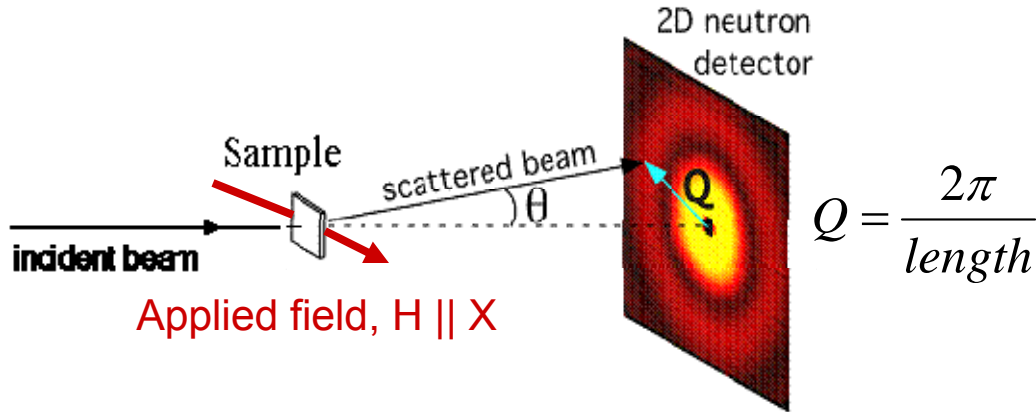


Throttled

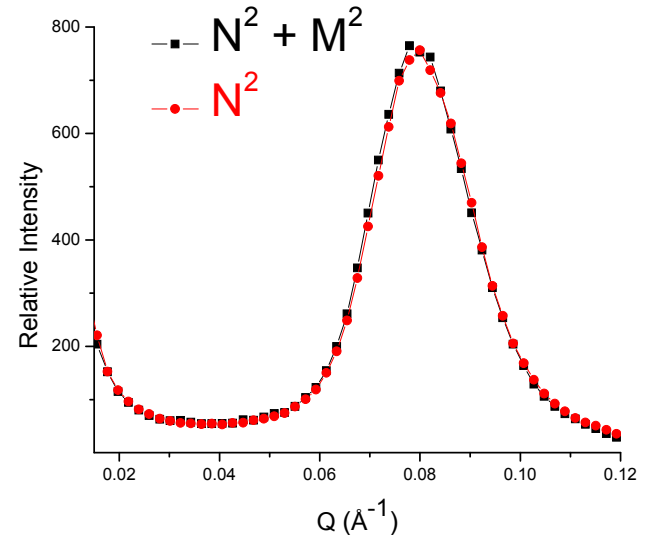
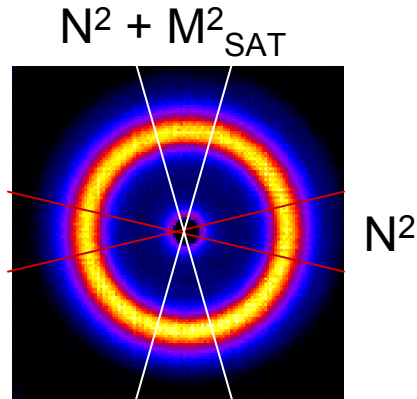
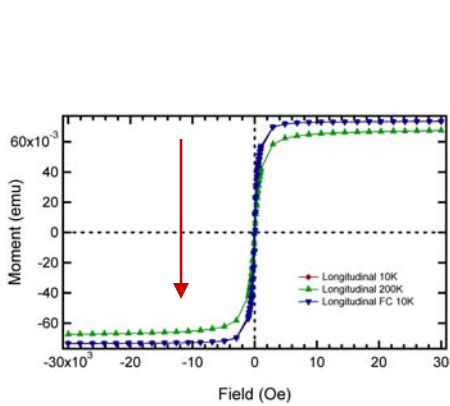
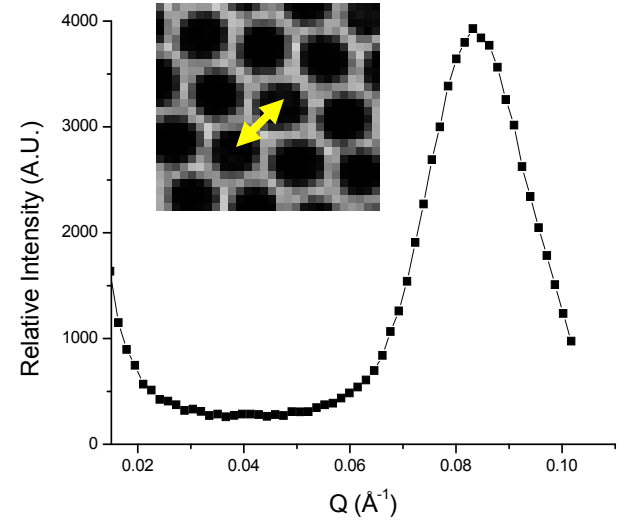
➤ Goal is to extend the polarized-analyzed SANS technique⁴ to probe magnetism with 3D sensitivity⁵ within any applied field.

1. S. Sun et al., J. Am. Chem. Soc. 126, 273 (2004)
2. P. Dutta et al., JAP 105, 07B510 (2009); J. Curiale et al., Appl. Phys. Lett. 95, 043106 (2009)
3. L. Berger et al., Phys. Rev. B 77, 104431 (2008); J. Mazo-Zuluaga et al., JAP 105, 123907 (2009)
4. T. R. Gentile et al., J. Appl. Crystallog. 33, 771 (2000); A. Wiedenmann et al., Physica B 356, 246 (2005); A.M. Gaspar et al., Biochim. Biophys. Acta. 1804, 76 (2010)
5. K. Krycka et al., Physica B, 404, 2561 (2009)

Small Angle Neutron Scattering (Unpolarized)



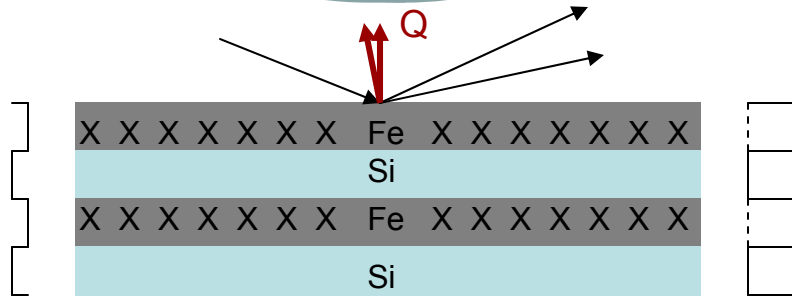
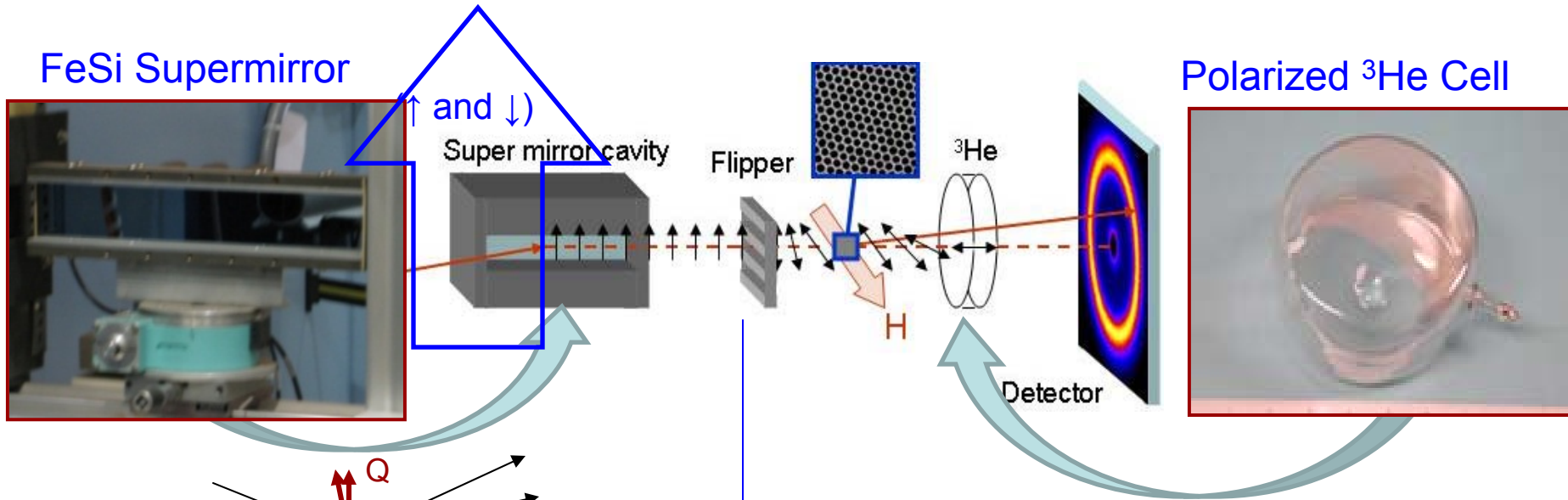
Neutrons magnetically scatter only from moments perpendicular to Q .



$$(\rho_M / \rho_N)^2 = 4\%$$

$$N, M_J(Q) = \sum_K \rho_{N, M_J}(K) e^{i\vec{Q} \cdot \vec{R}_K}$$

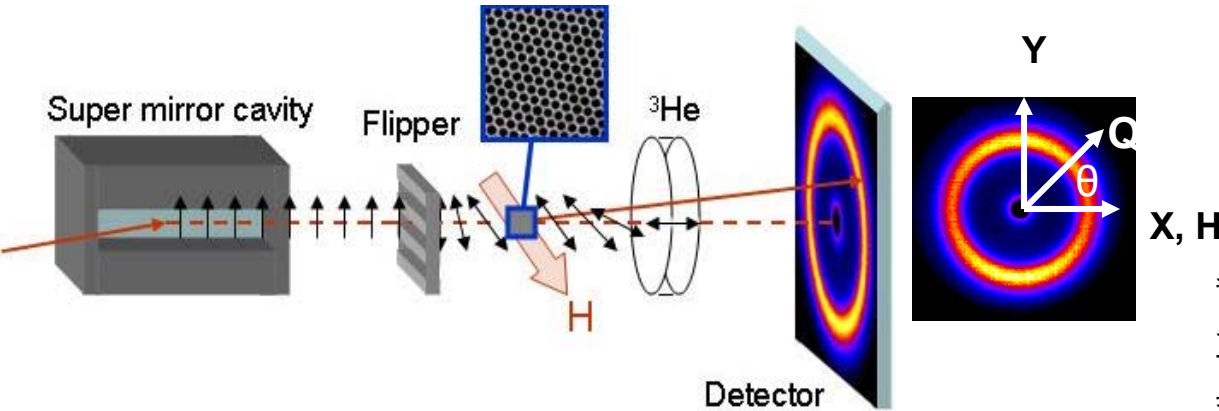
Set-Up for Polarization Analysis



$$I \propto |b_c \pm M|^2 = b_c^2 + M^2 \pm 2b_c M$$

- FeSi supermirror is stable and can achieve polarization of ~95%.
- Electromagnetic flipper is used to reverse polarization at will.

- Polarized ^3He allows spin-up neutrons of one orientation to pass while absorbing the opposite orientation.
- ^3He polarization can be reversed with NMR pulse.
- ^3He cells cover divergent beam, but have reduced transmission.

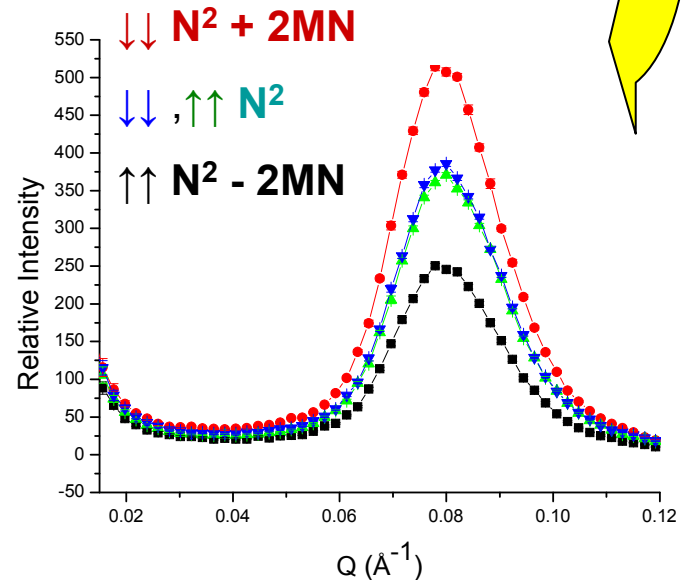
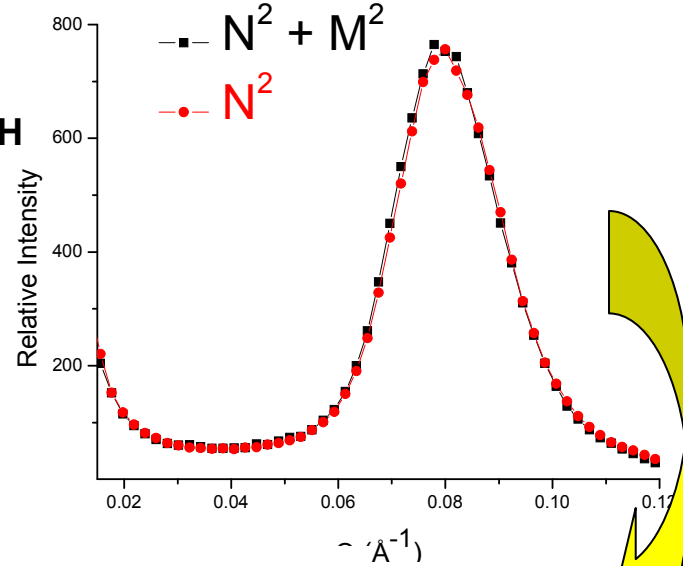


$$\vec{q} = \hat{M} - \hat{Q}(\hat{Q} \cdot \hat{M}) \Rightarrow q_A = \cos(\phi_{M,A}) - \cos(\phi_{Q,A}) \cos(\phi_{Q,M})$$

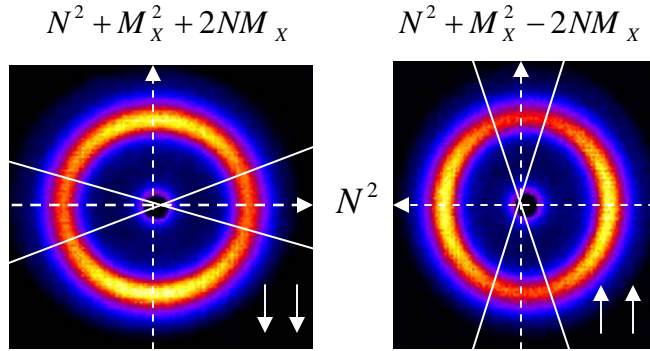
$$I^{\uparrow\uparrow, \downarrow\downarrow} \propto \left| \sum_j \rho_{n_j} e^{iQ \cdot R_j} \mp q_X \sum_k \rho_{m_{Xk}} e^{iQ \cdot R_k} \right|^2 = N^2 + q_X^2 M_X^2 \mp 2q_X N M_X$$

$$I^{\uparrow\downarrow, \downarrow\uparrow} \propto \left| q_Y \sum_j \rho_{m_j} e^{iQ \cdot R_j} \pm i q_Z \sum_k \rho_{m_{Hk}} e^{iQ \cdot R_k} \right|^2 = q_Y^2 M_Y^2 + q_Z^2 M_Z^2$$

From these eqns. we can separate N^2 , M_{PARL}^2 , and M_{PERP}^2 .

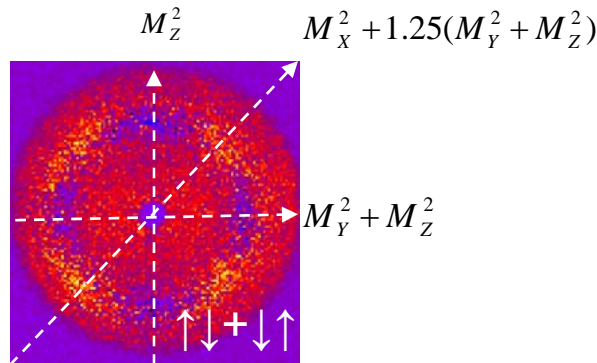
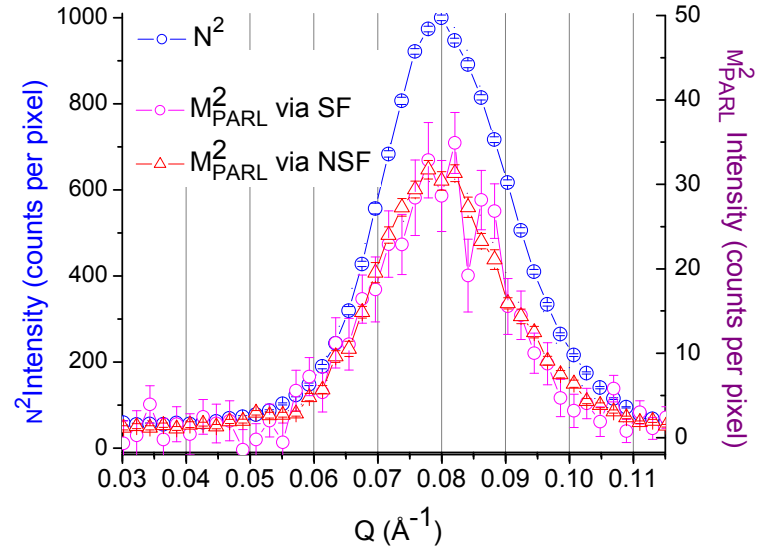


Scattering Profiles at 1.2 Tesla, 200 K



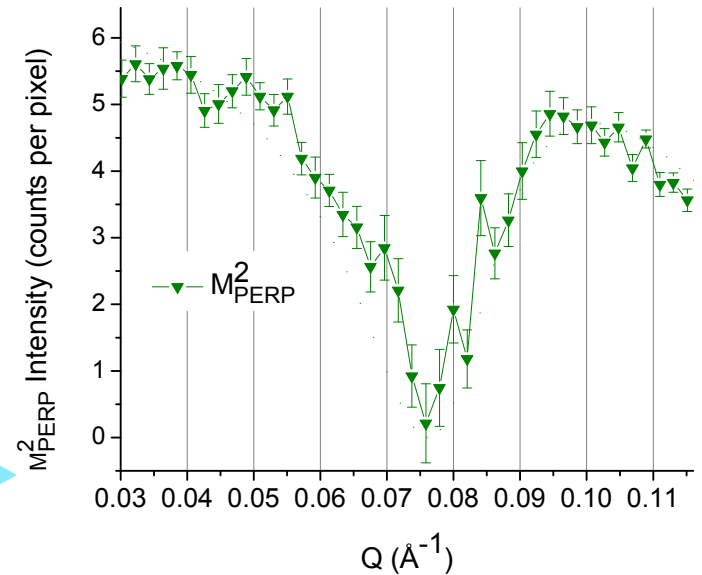
$$N^2 \propto (I_X^{\uparrow\uparrow} + I_X^{\downarrow\downarrow})$$

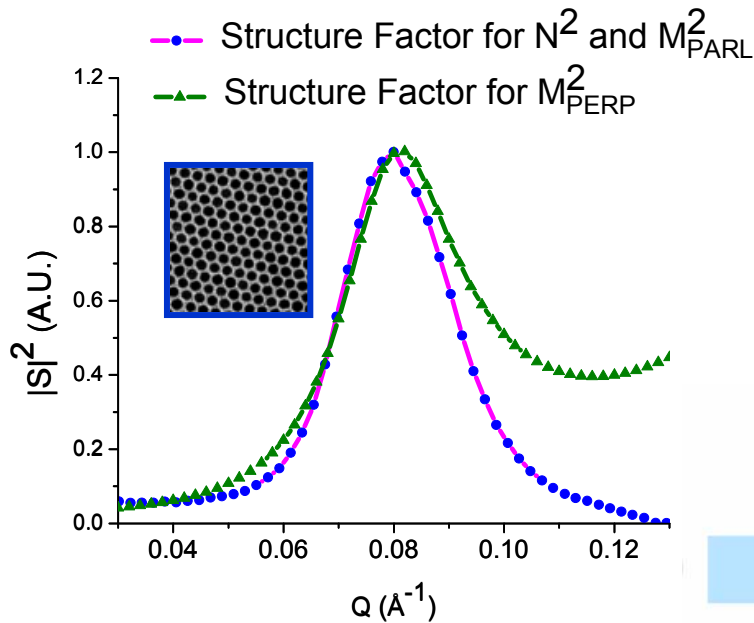
$$M_{PARL}^2 \propto (I_Y^{\downarrow\downarrow} - I_Y^{\uparrow\uparrow})^2 / 8N^2$$



$$M_{PARL}^2 = I_{45^\circ}^{\uparrow\downarrow, \downarrow\uparrow} - 1.25 M_{PERP}^2$$

$$M_{PERP}^2 = (I_X^{\uparrow\downarrow, \downarrow\uparrow} + I_Y^{\uparrow\downarrow, \downarrow\uparrow}) / 3$$

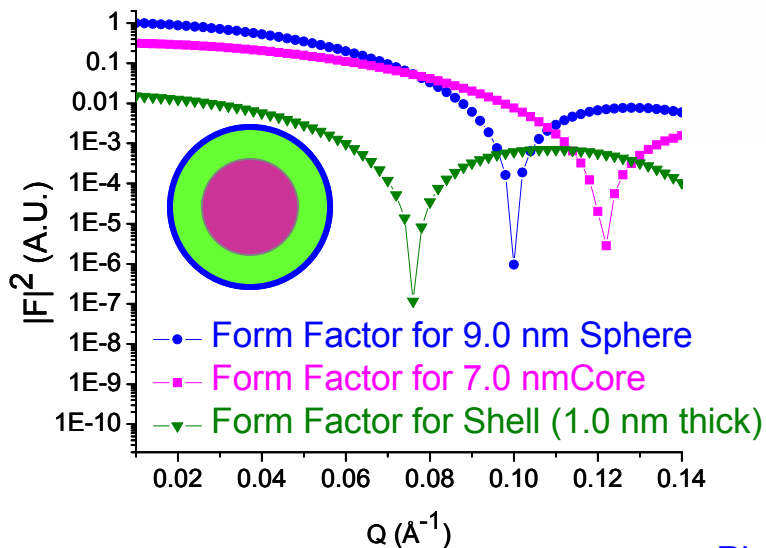
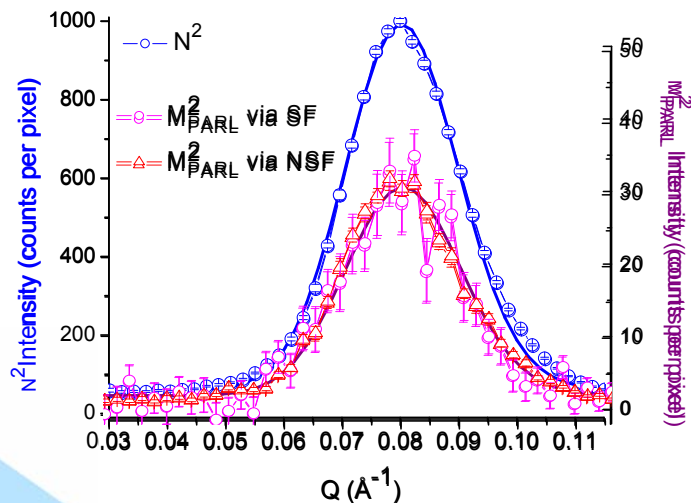
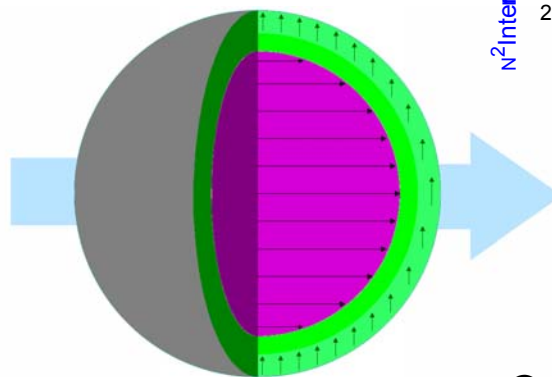




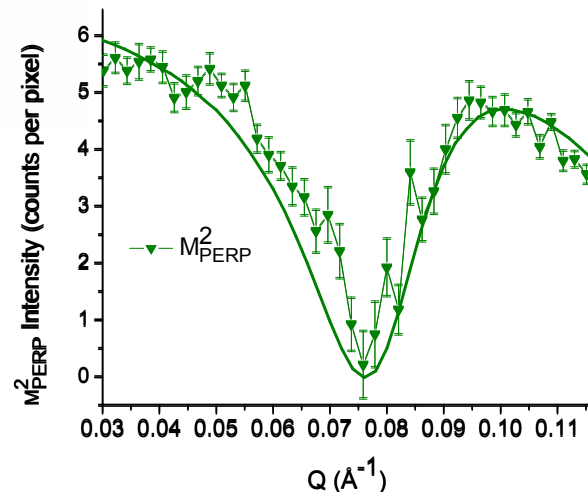
$$\rho_N = 6.97\text{E-}6 \text{ \AA}^{-2}$$

$$\rho_M = 1.46\text{E-}6 \text{ \AA}^{-2}$$

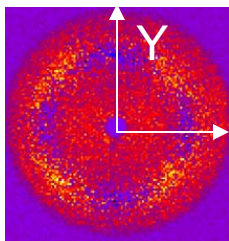
(513 emu / cc)



Modeled Diameters:
Sphere 9.0 nm
Ferrimagnetic core
7 nm
Canted shell 7 to 9
nm (± 0.2 nm)

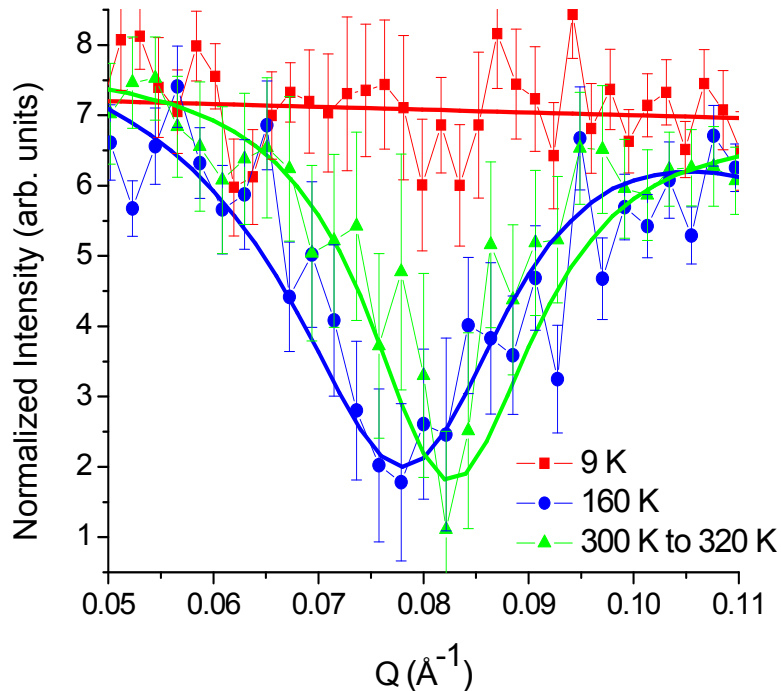


Altering Shell with Temperature at 1.2 Tesla



$$M_{PERP}^2 = (I_X^{\uparrow\downarrow, \downarrow\uparrow} + I_Y^{\uparrow\downarrow, \downarrow\uparrow}) / 3$$

X, H



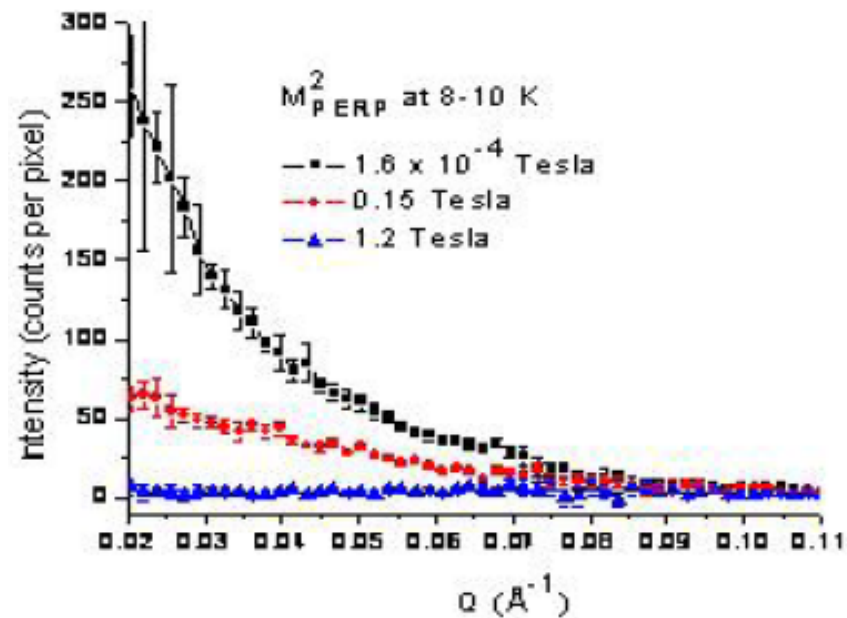
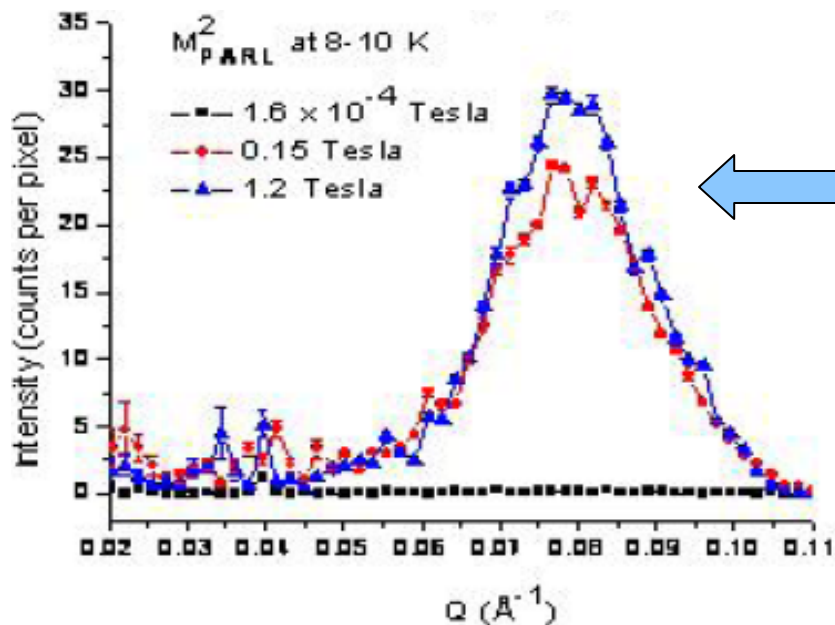
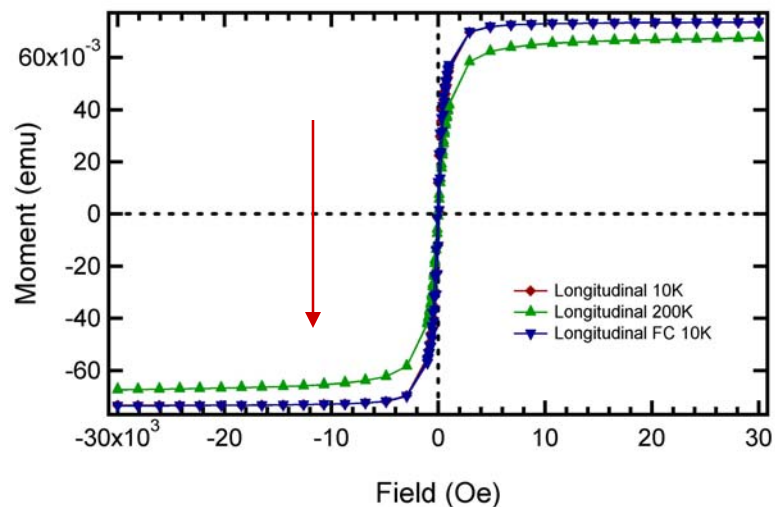
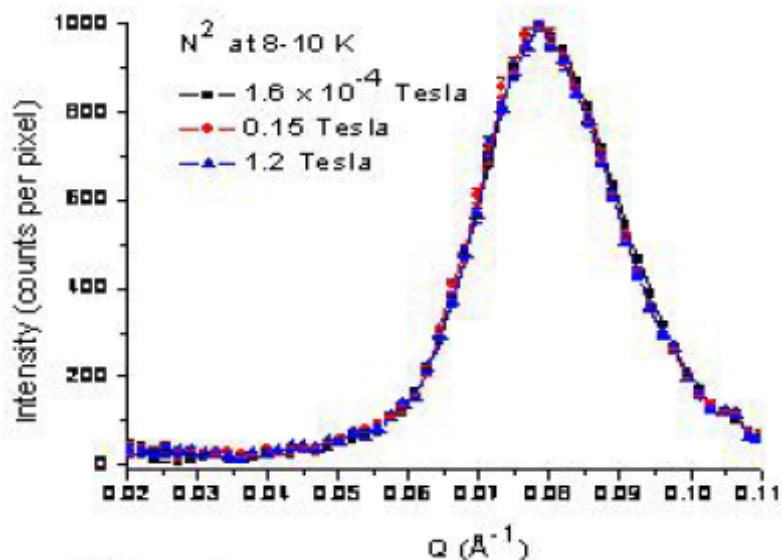
- 300-320 K dip at 0.082 Å⁻¹ comes from shell 1.5 nm thick (6 nm inner to 9 nm outer diameter)

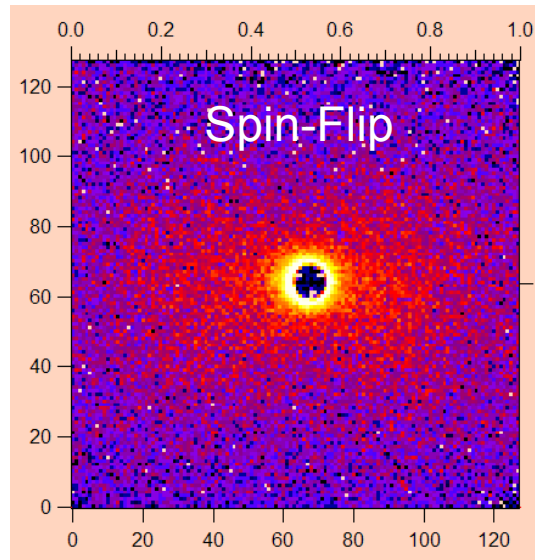
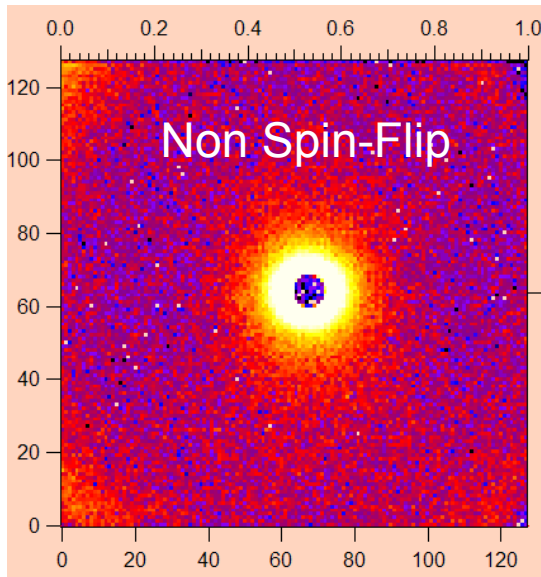
- 160 K dip at 0.075 Å⁻¹ comes from shell 1.0 nm thick (7 nm inner to 9 nm outer diameter)

- Field cooling to 10 K ($\ll T_{Block}$ @ 65 K) shows no signature of a canted shell

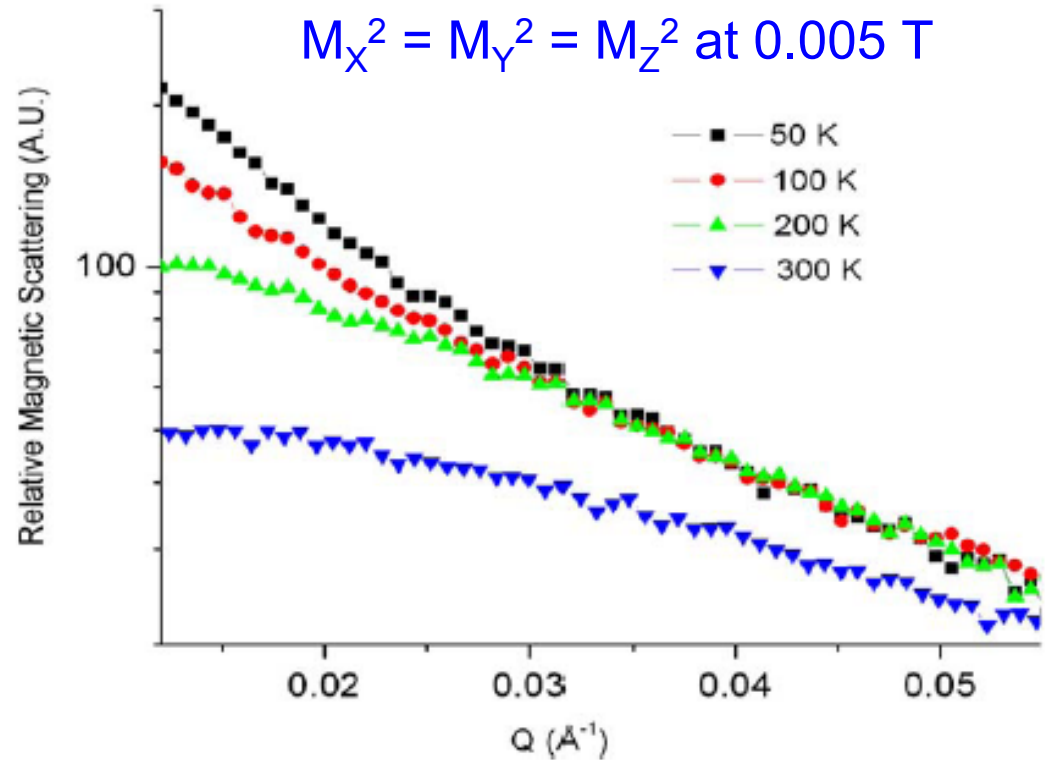
- Since M_{PARL}^2 scattering of similar magnitude at 10 K and 200 K, 1.2 Tesla, a disordered shell at 10 K is probable

Removal of field does not eliminate all magnetic scattering



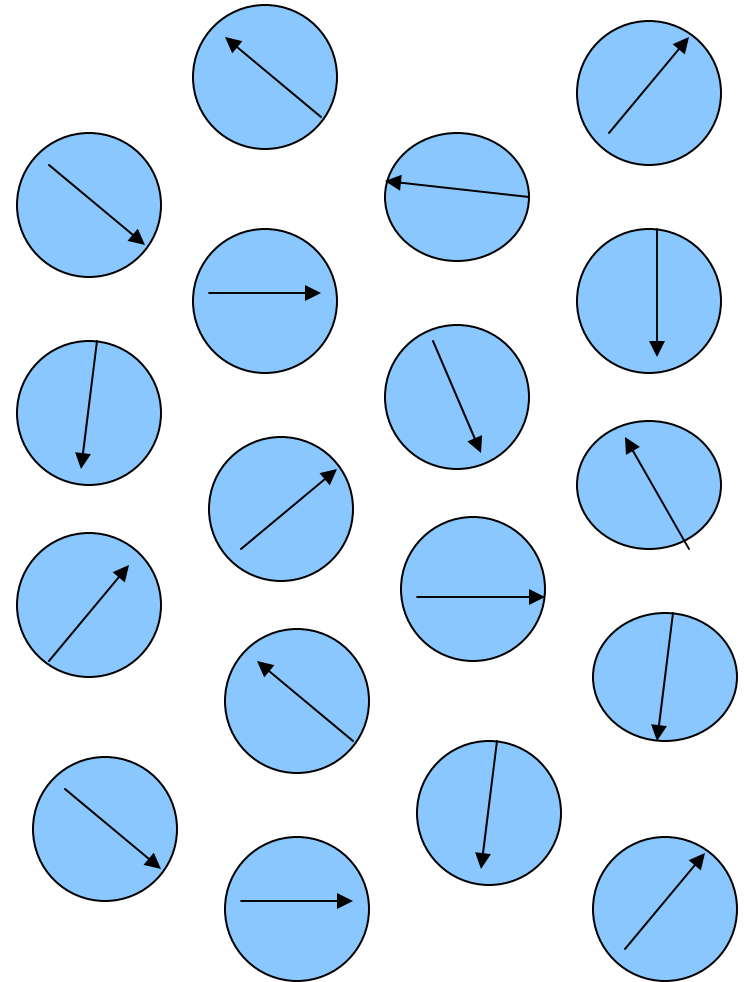
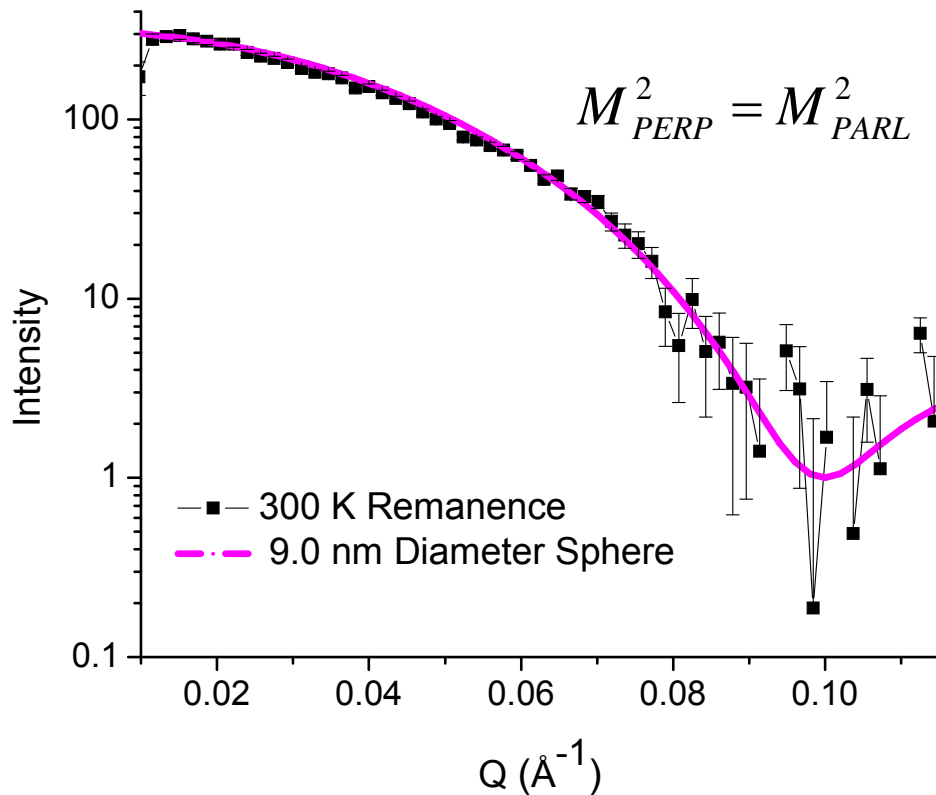


H →



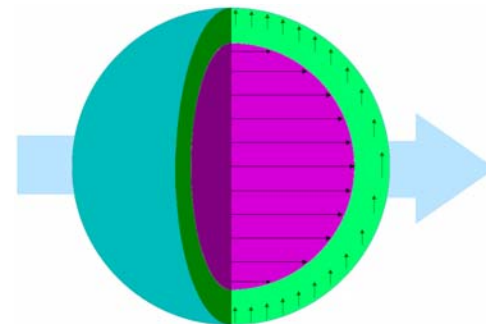
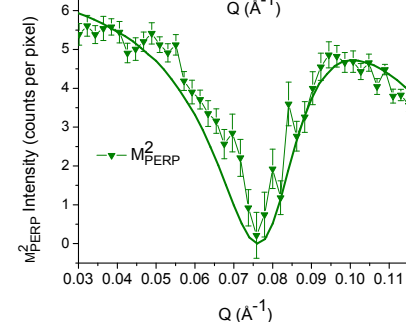
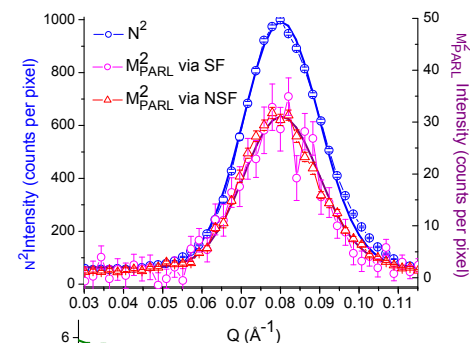
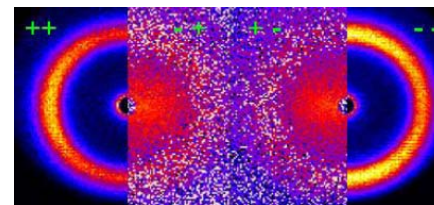
- Magnetic domains range from 1000 Å (~ 10 particles) at 50 K down to 100 Å (~ 1 particle) at 300 K

- Low-Q interparticle correlations virtually eliminated at 300 K, 0.005 T



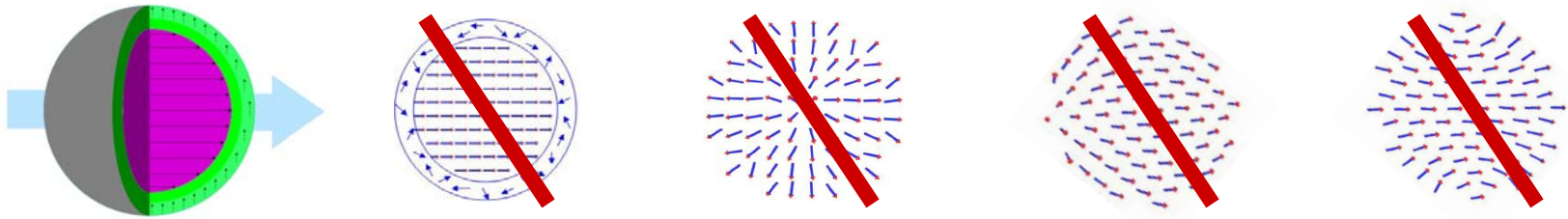
- Nanoparticles show no shell features and behave as uniform, ferrimagnetic spheres randomly oriented in space. **Thus, shell is magnetic in origin.**

- Direct evidence of canted magnetic shell 1.0 to 1.5 nm thick under high field between 160 and 320 K
- Zero-field cooling to 10 K eliminates ordered shell (though a disordered shell is probable)
- When field and interparticle interactions are removed (0.005 T, 300 K) the nanoparticles exhibit no shell morphology

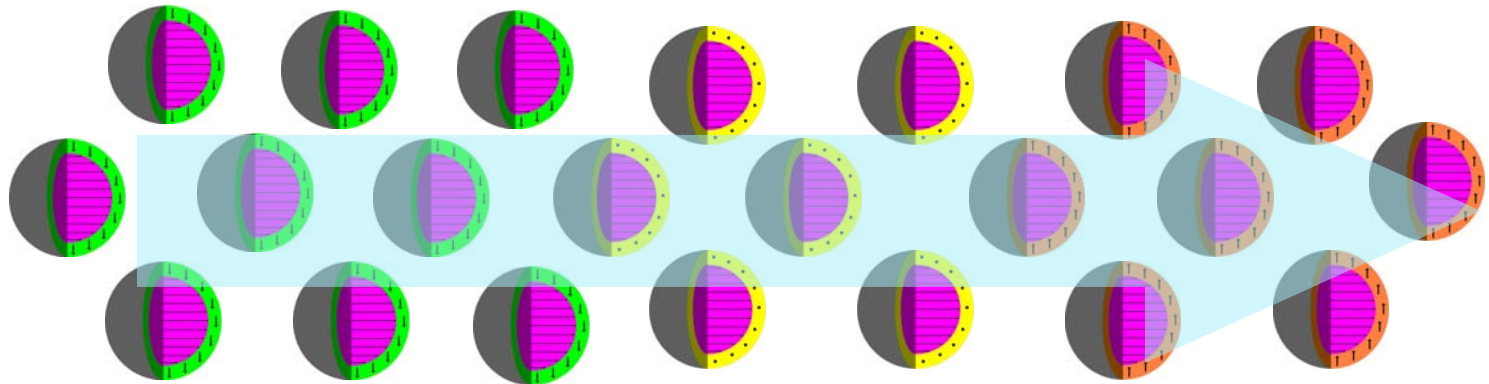


Possible origin of magnetic shell

- Discovery of canted magnetic shells exclude models involving disordered shells and those with radial symmetry at near-saturation conditions



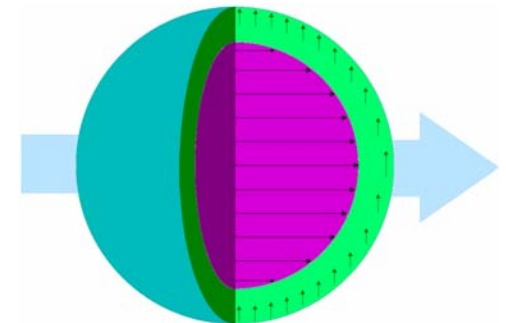
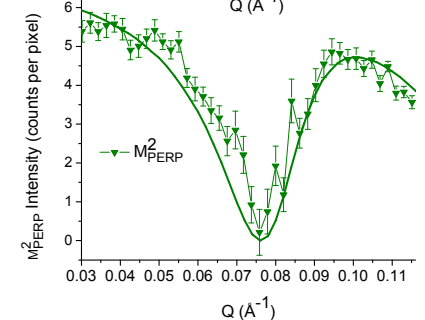
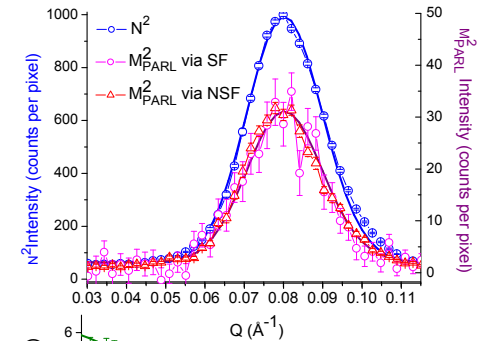
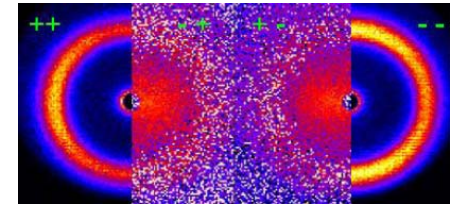
- Shells show correlations over one to several FCC lattice units, as seen by $|S|^2$.



- We speculate that the combination of surface anisotropy and interparticle coupling gives rise to the canted magnetic shells [J. Nogues et al., PRL 97, 157203 (2006); D. Kechrakos et al., JMMM 316, E291 (2007)]

- High-field temperature dependence (1.5 nm thick @ 300 K, 1.0 nm thick at 200 K, and missing or disordered at 9 K) is a mystery. Interparticle coupling changes with temperature and anisotropy may as well. There is a Verwey transition at 122 K and a bulk blocking temperature at 65 K.

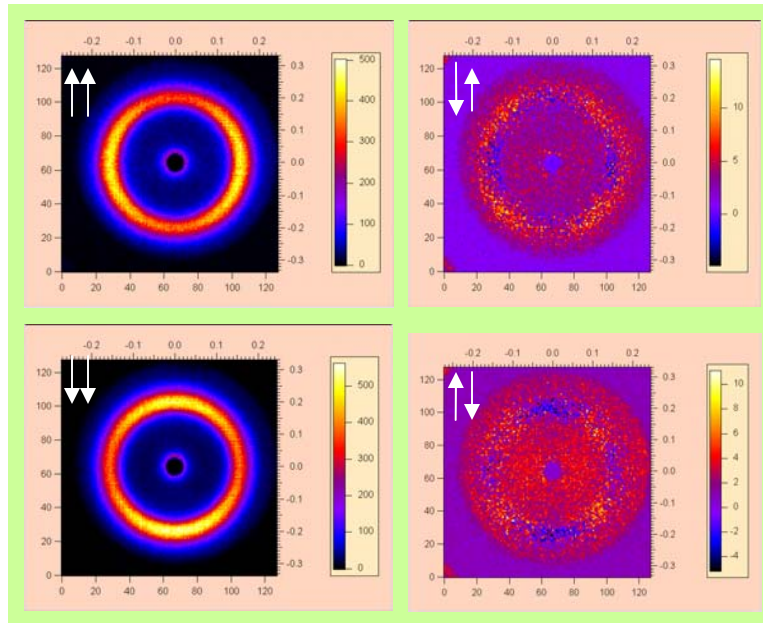
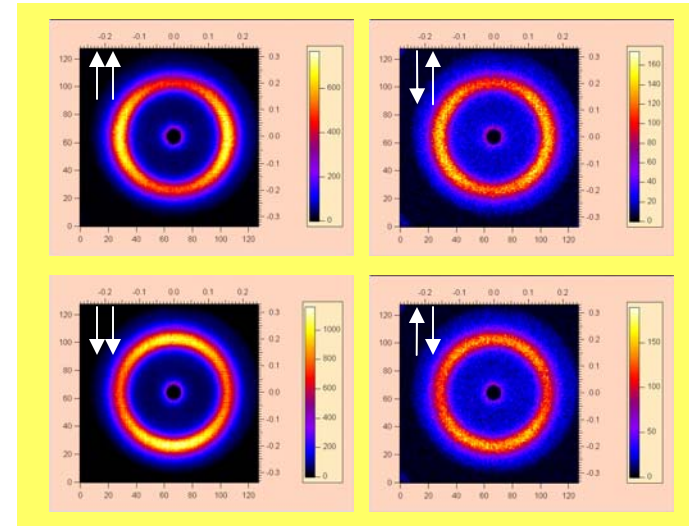
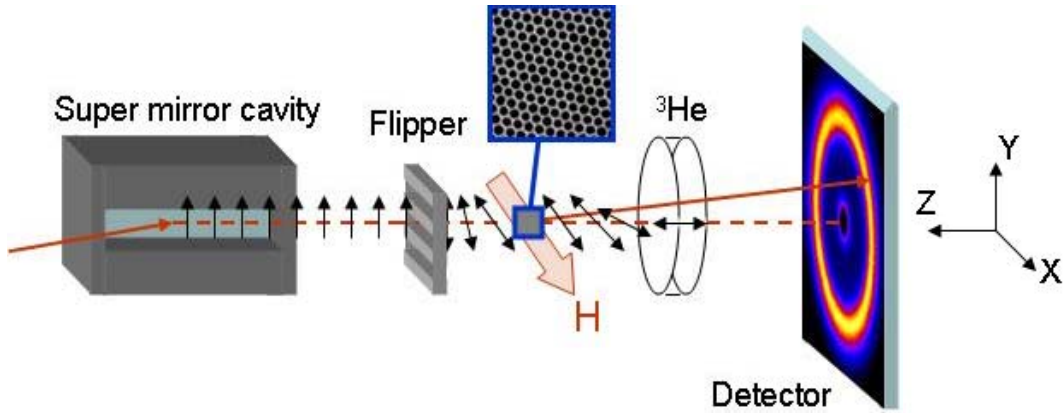
- Direct evidence of canted magnetic shell 1.0 to 1.5 nm thick under high field between 160 and 320 K
- Zero-field cooling to 10 K eliminates ordered shell (though a disordered shell is probable)
- When field and interparticle interactions are removed (0.005 T, 300 K) the nanoparticles exhibit no shell morphology
- Only with *polarization analyzed SANS* were we able to see details of perpendicular magnetic shells





THANK YOU

Correcting for Polarization Efficiencies



“user-friendly” polarization efficiency correction software

